

## Research Article

# Identification of swelling-activated $\text{Cl}^-$ current in rabbit cardiac Purkinje cells

A. O. Verkerk<sup>a,b,\*</sup>, R. Wilders<sup>a</sup> and J. H. Ravestloot<sup>a</sup>

<sup>a</sup> Department of Physiology, Room M01-09, Academic Medical Center, Meibergdreef 15, 1105 AZ Amsterdam (The Netherlands), Fax: +31 20 6919319, e-mail: a.o.verkerk@amc.uva.nl

<sup>b</sup> Experimental and Molecular Cardiology Group, Academic Medical Center, University of Amsterdam, Amsterdam (The Netherlands)

Received 20 January 2004; received after revision 17 February 2004; accepted 25 February 2004

**Abstract.** The presence and functional role of the swelling-activated  $\text{Cl}^-$  current ( $I_{\text{Cl(swell)}}$ ) in rabbit cardiac Purkinje cells was examined using patch-clamp methodology. Extracellular hypotonicity (210 or 135 mOsm) activated an outwardly rectifying, time-independent current with a reversal potential close to the calculated  $\text{Cl}^-$  equilibrium potential ( $E_{\text{Cl}}$ ). The magnitude of this current was related to tonicity of the superfusate. The current was blocked by 0.5 mM 4,4'-diisothiocyanostilbene-2,2'-disulfonic acid (DIDS). These features are comparable to

those of  $I_{\text{Cl(swell)}}$  found in sinoatrial nodal, atrial, and ventricular myocytes.  $I_{\text{Cl(swell)}}$  activation at 210 and 135 mOsm depolarized the resting membrane potential with 6 and 10 mV and shortened the action potential by ~18 and ~33 %, respectively. DIDS partially reversed  $I_{\text{Cl(swell)}}$ -induced action potential changes. We conclude that  $I_{\text{Cl(swell)}}$  is present in Purkinje cells and its activation leads to action potential shortening and resting membrane potential depolarization, both of which can promote the development of reentrant arrhythmias.

**Key words.** Purkinje cell; osmotic stress; chloride channel; action potential; ectopic activity.

A swelling-activated  $\text{Cl}^-$  current ( $I_{\text{Cl(swell)}}$ ) has been described in a variety of cardiac cells of different mammalian species, including atrium and ventricle of dog [1, 2], rabbit [3, 4], guinea pig [5], human [6], and sinoatrial node (SAN) node of rabbit [3].  $I_{\text{Cl(swell)}}$  is an outwardly rectifying current, which activates after cells have been exposed to hypotonic solutions [1, 2], or a raised cytoplasmic hydrostatic pressure [3]. Activation of  $I_{\text{Cl(swell)}}$  occurs in an osmotic gradient-dependent fashion [7, 8] with a distinct lag after changes in cell size [9].  $I_{\text{Cl(swell)}}$  is time independent within the physiological range of potentials, but exhibits relaxation or inactivation at extreme positive potentials [10].

In cardiac cells, the normal intracellular  $\text{Cl}^-$  concentration is around 20 mM. Estimations of the  $\text{Cl}^-$  equilibrium potential ( $E_{\text{Cl}}$ ) thus range from –40 to –60 mV [11, 12]. Therefore,  $I_{\text{Cl(swell)}}$  is an outwardly directed, repolarizing current during phase 1 and phase 2 of the cardiac action potential. During these phases,  $I_{\text{Cl(swell)}}$  would cause action potential shortening, which was indeed shown in ventricular cells of guinea pig [13] and rabbit [8, 14].  $I_{\text{Cl(swell)}}$  is an inwardly directed, depolarizing current at resting membrane potentials. Its action would result in depolarization of the resting membrane potential (RMP), which was shown in rabbit SAN cells [15, 16], dog atrial cells [17], and in ventricular cells of guinea pig [13], rabbit [8, 14], and dog [17]. In addition, activation of  $I_{\text{Cl(swell)}}$  decreases the spontaneous beating rate in SAN cells [15, 16]. Recently,  $I_{\text{Cl(swell)}}$  was demonstrated to be persistently

\* Corresponding author.

active under basal, isosmotic conditions in cells isolated from hypertrophied hearts of rat and dog [7, 18], although this is not consistent with findings in rabbit [8]. These findings thus indicate that  $I_{Cl(swell)}$  may play a role in the electrophysiology of SAN, atrial, and ventricular cells under pathophysiological conditions.

To date, the presence and properties of  $I_{Cl(swell)}$  in cardiac Purkinje cells are unknown. The present study was designed to address this issue. We exposed single rabbit Purkinje cells to hypotonic bathing solutions of 210 or 135 mOsm. Here we report that the consequent cell swelling activates a time-independent, outwardly rectifying current with a reversal potential close to the calculated  $E_{Cl}$ . The current was reversibly blocked by 0.5 mM 4,4'-diisothiocyanostilbene-2,2'-disulfonic acid (DIDS), a well-known  $Cl^-$  current blocker [19, 20]. The hypotonic solutions caused action potential shortening and RMP depolarization. These effects on action potential configuration were attenuated by DIDS. All of the aforementioned features of the swelling-induced current we found in rabbit Purkinje cells are shared with  $I_{Cl(swell)}$  found in SAN, atrial, and ventricular cells [for reviews, see refs 19–21]. We thus conclude that  $I_{Cl(swell)}$  is present in cardiac Purkinje cells of the rabbit.

## Materials and methods

### Solutions and drugs

Normal Tyrode's solution contained (in mM): NaCl 140, KCl 5.4,  $CaCl_2$  1.8,  $MgCl_2$  1.0, glucose 5.5, and HEPES 5.0; pH was adjusted to 7.4 with NaOH. The Kraft-Brühe (KB) solution contained (in mM): KCl 85,  $K_2HPO_4$  30,  $MgSO_4$  5.0, glucose 20, pyruvic acid 5.0, creatine 5.0, taurine 5.0, EGTA 0.5,  $\beta$ -hydroxybutyric acid 5.0, succinic acid 5.0, and  $Na_2$ -ATP 2.0; pH was adjusted to 7.2 with KOH. The pipette solution contained (mM): K-glucuronate 136, KCl 9.2,  $K_2$ -ATP 5, HEPES 10; pH was adjusted to 7.2 with KOH. The composition of the pipette solution was chosen such that the  $E_{Cl}$  was  $-50$  mV, close to the physiological value when the cells are bathed in the modified Tyrode's solutions with reduced NaCl concentrations (see below). Osmolarity of the pipette solution was  $\sim 260$  mOsm.

DIDS (Sigma, St. Louis, Mo.) was prepared as an 0.5 M stock solution in DMSO and protected from bright light. DIDS stock solution was diluted just before the experiments to a final concentration of 0.5 mM.

### Cell preparation

Single cardiac Purkinje cells were isolated from hearts of New Zealand White rabbits (3.5–4.5 kg) by an enzymatic dissociation procedure modified from Verkerk et al. [22]. Hearts were quickly removed from anesthetized rabbits (1 ml/kg Hypnorm). Free-running Purkinje

strands, free from ventricular tissue, were excised from the left ventricle and placed in the following solutions: (1) 20 min in nominally  $Ca^{2+}$ -free Tyrode's solution in which 1 mg/ml protease (220 U/L type XIV; Sigma) and 1 mg/ml bovine serum albumin (BSA; Behring, Marburg, Germany) were dissolved; (2) 20 min in nominally  $Ca^{2+}$ -free Tyrode's solution to which 1 mM EGTA was added, and (3) 15–30 min in nominally  $Ca^{2+}$ -free Tyrode's solution in which 0.2 mg/ml protease, 0.5 mg/ml collagenase (59 U/L type B; Boehringer, Mannheim, Germany), 0.5 mg/ml BSA, and 0.2 mM EGTA were dissolved. To obtain single Purkinje cells, the strands were agitated for 5–10 min by a magnetic stirring bar at 120–150 rpm in KB solution. Next, the KB solution was placed in a disposable centrifuge tube in which the single cells were allowed to sediment. Finally, the KB solution was replaced with normal Tyrode's solution in three steps. In each step, approximately 75% of the solution on top of the cells was carefully replaced with Tyrode's solution. The time interval between the solution changes was 15–20 min. The temperature of all solutions used for the isolation procedure was maintained at 36–37°C. The cells were stored at room temperature (20–22°C) and used within 8 h after isolation.

### Recording procedures and patch-clamp protocols

(1) Recording procedures. Small aliquots of cell suspension were put in a recording chamber on the stage of a Nikon inverted microscope. The cells were allowed to sediment and adhere for 5 min after which continuous perfusion with normal Tyrode's solution (36–37°C) was started. Rod-shaped cells with smooth surfaces were selected for electrophysiological measurements. Membrane potentials and currents were recorded in the ruptured patch whole-cell configuration of the patch-clamp technique using a custom-made voltage-clamp amplifier. Patch pipettes were pulled from borosilicate glass and heat polished. All potentials were corrected for the calculated liquid junction potential ( $-13$  mV). Membrane currents and potentials were filtered on-line (1 kHz), digitized at 2 kHz, stored and analyzed by custom-made software run on an Apple PowerMac personal computer.

(2) Current-clamp experiments. Action potentials were elicited at a frequency of 1 Hz by current pulses of 2 ms applied via the patch pipette. The following action potential parameters were measured: action potential duration at 20% repolarization ( $APD_{20}$ ), action potential duration at 50% repolarization ( $APD_{50}$ ), action potential duration at 90% repolarization ( $APD_{90}$ ), RMP, and action potential amplitude (APA). Cell capacitance ( $C_m$ ) was calculated as  $C_m = \Delta I_m / \Delta(dV_m/dt)$ , where  $\Delta(dV_m/dt)$  is the change in initial slope of the membrane potential ( $V_m$ ) upon 10-ms hyper- and depolarizing pulses of 100 pA ( $\Delta I_m$ ) applied during the action potential plateau [22].

(3) Voltage-clamp experiments. The 'quasi steady-state' current ( $I_{qss}$ ) was measured as the current at the end of 500-ms steps to voltages ranging from  $-110$  mV to  $+50$  mV with  $10$  mV increments at a frequency of  $0.5$  Hz. The holding potential was  $-50$  mV.  $I_{qss}$  was normalized for cell size by dividing current amplitude by cell capacitance.

(4) Purkinje cell characterization. The cells used in this study were clearly identified as Purkinje cells on the basis of origin, morphology, and some of their electrical properties [23, 24]. First, the cells were isolated from free-running Purkinje strands, which were free from ventricular tissue. Second, under light microscopy, the Purkinje cells typically showed a narrower and longer morphology with much less prominent cross-striations compared to ventricular myocytes. Third, action potential upstroke velocity was higher, but the current density of the inward rectifier current ( $I_{K1}$ ) was smaller compared to ventricular cells (data not shown), consistent with previous findings in rabbit Purkinje cells [23, 24].

In single sheep Purkinje cells as well as intact Purkinje strands of sheep, dog, and baboon, two distinct types of action potential configuration are present [22, 25–27]. In our previous study [22], we found that about 50% of the single sheep Purkinje cells showed action potentials with a prominent phase 1 repolarization and relatively negative plateau ('low-plateau' Purkinje cells), whereas the remaining single cells had little phase 1 repolarization and a relatively positive plateau ('high-plateau' Purkinje cells). Whether single rabbit Purkinje cells also show two types of action potential is not yet known. In the present study, the action potential plateau levels varied considerably, preventing us from drawing conclusions regarding the existence of two distinct types of action potential in single rabbit Purkinje cells.

### Hypotonicity

To induce cell swelling, the cells were superfused with 'modified' Tyrode's solutions with an osmolality of  $\sim 300$  mOsm,  $\sim 210$  mOsm, or  $\sim 135$  mOsm as described previously in detail [8]. In the modified Tyrode's solutions, the NaCl concentration of the normal Tyrode's solution was lowered to  $55$  mM and sucrose was added to obtain the desired osmolality. A freezing-point depression-type osmometer (Knauer, Germany) was used routinely to verify tonicity of all solutions used. Despite the lowered NaCl concentration and reduced ionic strength of our sucrose-containing, modified Tyrode's solutions, Purkinje cells proved capable of producing action potentials. However, switching from normal Tyrode's solution to its modified isosmotic,  $300$ -mOsm, variant changed the action potential configuration significantly (table 1). Although the osmolalities were similar, the reduction in NaCl concentration resulted in action potential shortening, APA reduction, and RMP hyperpolarization, which

Table 1. Action potential characteristics of rabbit Purkinje cells ( $n = 16$ ) in normal Tyrode's solution and in modified Tyrode's solution of  $300$  mOsm.

	Normal Tyrode's solution	Modified Tyrode's solution
APD <sub>20</sub> (ms)	$80 \pm 17$	$44 \pm 8^*$
APD <sub>50</sub> (ms)	$162 \pm 26$	$104 \pm 15^*$
APD <sub>90</sub> (ms)	$235 \pm 19$	$184 \pm 13^*$
RMP (mV)	$-80 \pm 2$	$-86 \pm 2^*$
APA (mV)	$117 \pm 4$	$112 \pm 3^*$

Values are the mean  $\pm$  SE. APD<sub>20</sub>, APD<sub>50</sub>, and APD<sub>90</sub>, action potential duration at 20, 50, and 90% repolarization, respectively; RMP, resting membrane potential; APA, action potential amplitude. \* $p < 0.05$ .

agrees with previous findings in ventricular cells [8]. The underlying ionic mechanism was not investigated, but may be related to changes in electrogenic  $Na^+$  transport systems, i.e., non-inactivating  $Na^+$  current,  $Na^+$ - $K^+$  pump, and  $Na^+$ - $Ca^{2+}$  exchange current. In any case, by reducing the sucrose concentration of the modified Tyrode's solutions, osmolality could be changed without affecting all other ionic conditions any further, whereupon the effects of cell swelling on the electrophysiological properties of rabbit Purkinje cells could be studied.

### Statistics

Values are expressed as the mean  $\pm$  SE. Two data sets were considered significantly different if the  $P$  value of the analysis of variance (ANOVA) or Student's  $t$  test was less than  $0.05$ . Action potential parameters were obtained from ten consecutive action potentials and averaged.

## Results

### Effects of extracellular hypotonicity on action potential configuration

Exposure of Purkinje cells to hypotonic bathing solutions invariably led to a drastic shortening of the action potential and RMP depolarization. Figure 1 shows typical examples of these electrophysiological effects of an extracellular tonicity of  $135$  mOsm (fig. 1A, B) and  $210$  mOsm (fig. 1C, D). After a latency of several hundreds of seconds, the hypotonic bathing solutions caused a gradual decline in APD<sub>90</sub> and an equally gradual RMP depolarization (fig. 1A, C). Phase 1 and phase 2 repolarization accelerated, but late during phase 3, repolarization decelerated (fig. 1B, D), the net effect being a clear action potential shortening. Upon restoring isotonicity, both APD<sub>90</sub> and RMP returned to control values, or almost so. Table 2 summarizes the data of these two cells as well as 14 others. APD<sub>90</sub> was reduced by  $\sim 10\%$  when the cells were exposed to an extracellular tonicity of  $210$  mOsm, but by as much as  $\sim 30\%$  when extracellular tonicity was

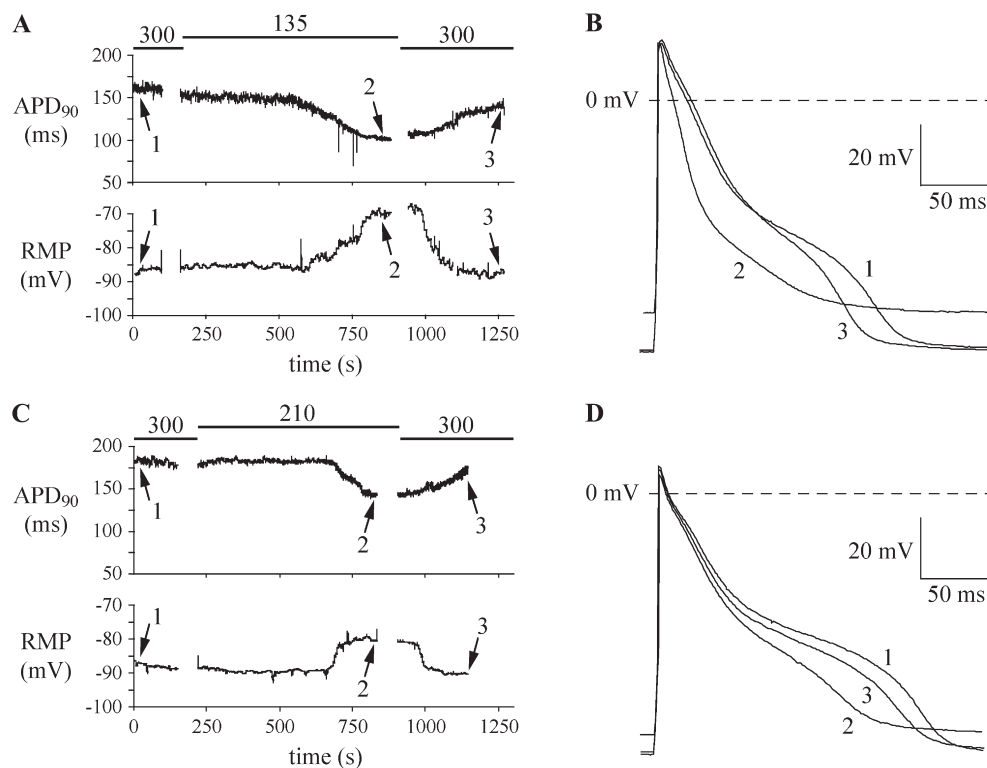


Figure 1. (A) Simultaneous recordings of action potential duration measured at 90% repolarization (APD<sub>90</sub>; top) and resting membrane potential (RMP; bottom) before, during, and after application of the 135-mOsm hypotonic bathing solution. The action potential measurements were alternated by periods in which the cell was voltage clamped. (B) Action potentials recorded at the times indicated by arrows in A. (C) Time course of changes in APD<sub>90</sub> (top) and RMP (bottom) before, during, and after application of the hypotonic bathing solution of 210 mOsm. (D) Action potentials recorded at the times indicated by arrows in C.

Table 2. Action potential characteristics of rabbit Purkinje cells in modified Tyrode's solution of 135 mOsm (n = 9) and 210 mOsm (n = 7).

	300 mOsm	135 mOsm	300 mOsm	210 mOsm
APD <sub>20</sub> (ms)	41 ± 14	25 ± 9*	47 ± 6	38 ± 6*,†
APD <sub>50</sub> (ms)	109 ± 27	63 ± 15*	100 ± 11	76 ± 10*,†
APD <sub>90</sub> (ms)	186 ± 19	131 ± 19*	181 ± 17	159 ± 17*,†
RMP (mV)	-86 ± 3	-76 ± 2*	-85 ± 2	-79 ± 3*,†
APA (mV)	113 ± 5	107 ± 6*	111 ± 2	101 ± 4*

Values are the mean ± SE. APD<sub>20</sub>, APD<sub>50</sub>, and APD<sub>90</sub>, action potential duration at 20, 50, and 90% repolarization, respectively; RMP, resting membrane potential; APA, action potential amplitude. \*p < 0.05 vs 300 mOsm; †p < 0.05 vs 135 mOsm.

135 mOsm. A similar osmotic gradient dependency was found for the hypotonicity-induced RMP depolarization. RMP depolarized by ~6 mV when the cells were exposed to an extracellular tonicity of 210 mOsm, and by ~10 mV when extracellular tonicity was 135 mOsm.

#### Effects of extracellular hypotonicity on quasi steady-state current

Our current-clamp experiments show that extracellular hypotonicity, after a latency of a few minutes, causes action potential shortening and RMP depolarization. To determine what current provokes these changes, action po-

tential measurements were interrupted and the same Purkinje cells were subjected to a voltage-clamp protocol. Depolarizing and hyperpolarizing voltage-clamp steps of 500-ms duration were applied from a holding potential of -50 mV. Figure 2A shows typical examples of current traces recorded at -100, -50, 0, and +50 mV when the cells were exposed to the modified, sucrose-containing, 300-mOsm Tyrode's solution (left panel) and the 135-mOsm (middle panel) variant. During the hypotonic bathing,  $I_{qss}$  was increased at all potentials, except -50 mV. The increase at very positive potentials (+50 mV), however, was larger than at very negative po-

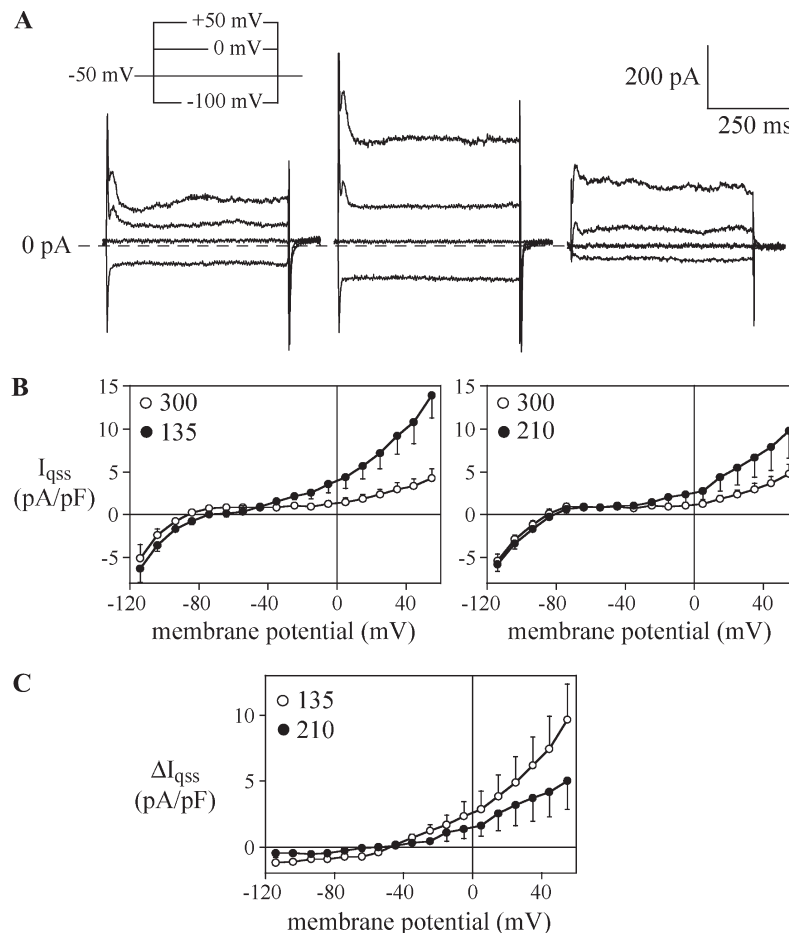


Figure 2. (A) Current traces recorded at  $-100$ ,  $-50$ ,  $0$ , and  $+50$  mV at  $300$  mOsm (left) and  $135$  mOsm (middle), and the hypotonicity-induced current constructed by subtracting current traces recorded at  $300$  mOsm from those recorded at  $135$  mOsm (right). (B) Current-voltage (I-V) relationships of quasi steady-state current ( $I_{qss}$ ) under isotonic conditions ( $300$  mOsm) and at  $135$  mOsm (left;  $n = 7$ ) and  $210$  mOsm (right;  $n = 7$ ). (C) I-V relationship of the change in current induced by the hypertonic solutions ( $\Delta I_{qss}$ ) of  $135$  mOsm ( $n = 7$ ) and  $210$  mOsm ( $n = 7$ ) from a starting osmolarity of  $300$  mOsm.

tentials ( $-100$  mV). By digitally subtracting the current traces recorded under  $135$ -mOsm hypotonic conditions from those recorded under  $300$ -mOsm isosmotic conditions, the hypotonicity-induced difference current was obtained (fig. 2A, right panel). The difference current is time independent, except at very positive potentials ( $+50$  mV) where it shows a moderate decline. Figure 2B summarizes the I-V relationships of  $I_{qss}$  recorded during the modified, sucrose-containing,  $300$ -mOsm Tyrode's solution and the  $135$ -mOsm (left;  $n = 7$ ), and  $210$ -mOsm (right;  $n = 7$ ) variants. Figure 2C shows the I-V relationships of the hypotonicity-induced difference current ( $\Delta I_{qss}$ ) at  $135$  and  $210$  mOsm (open and closed circles, respectively). Both relationships show a clear outward rectification. The reversal potential of the difference current is approximately  $-50$  mV, which is close to the calculated  $E_{Cl}$ . Finally, the magnitude of the hypotonicity-induced difference current is proportional to the osmotic gradient. These findings are consistent with activation of  $I_{Cl(swell)}$  [for reviews, see refs 19–21].

### Effects of blocking $I_{Cl(swell)}$

The stilbene derivative DIDS is a well-known blocking agent of  $I_{Cl(swell)}$  [19, 20]. To further ascertain the identity of the hypotonicity-induced membrane currents, we studied the effects of  $0.5$  mM DIDS in three swollen rabbit Purkinje cells. In these experiments,  $10$  mM EGTA was added to the pipette solution to block the  $Ca^{2+}$ -activated  $Cl^-$  current [28]. Figure 3A shows a representative example of  $I_{qss}$  recorded at  $-100$  and  $+50$  mV when the extracellular tonicity was  $300$  and  $135$  mOsm (open and closed circles, respectively). At a dose of  $0.5$  mM, DIDS virtually completely blocked the effects of the hypotonic solution on  $I_{qss}$  (triangles). This effect was consistently observed in all cells tested. When active, time-independent currents that reverse around  $-50$  mV tend to abbreviate action potential duration and depolarize RMP, as we observed in our current clamp experiments with swollen Purkinje cells (fig. 1B, D). If the changes in the current clamp properties of swollen cells are largely due to  $I_{Cl(swell)}$ , DIDS should attenuate these. The effects of DIDS on action potentials during hypotonicity were



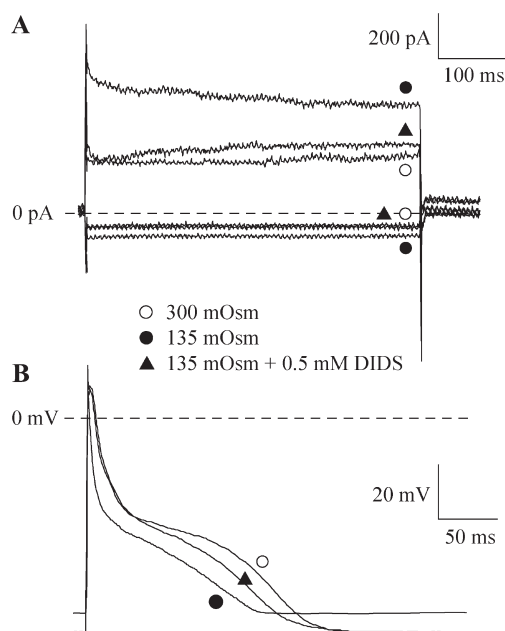


Figure 3. (A) Effects of 0.5 mM DIDS on hypotonicity-induced changes in quasi steady-state current at  $-100$  and  $+50$  mV (bottom and top traces, respectively). (B) Effects of 0.5 mM DIDS on hypotonicity-induced changes in action potential configuration.

studied in three Purkinje cells with 10 mM EGTA in the pipette. Figure 3B shows action potentials recorded from a Purkinje cell when the extracellular tonicity was 300 and 135 mOsm (open and closed circles, respectively). Application of 0.5 mM DIDS indeed reversed the effects of the hypotonic solution to a large extent (triangles). This effect was consistently observed in all cells tested. From these experiments we conclude that  $I_{Cl(swell)}$  underlies the action potential changes provoked by hypotonicity.

## Discussion

### $I_{Cl(swell)}$ is present in cardiac Purkinje cells

SAN, atrial, and ventricular cells from different species have been demonstrated to express a swelling-activated chloride current. Its presence in cardiac Purkinje cells was unknown. In this study, we employed patch-clamp methodology to investigate the presence of  $I_{Cl(swell)}$  in cardiac Purkinje cells of rabbit. Our voltage-clamp experiments showed that cell swelling induced by hypotonic bathing solutions of 135 and 210 mOsm activated an outwardly rectifying membrane current with a reversal potential close to  $E_{Cl}$  (fig. 2C). The current appeared after a delay of a few minutes. It proved sensitive to DIDS (fig. 3A) and the current density was proportional to the osmotic gradient (fig. 2C). These features closely resemble those of  $I_{Cl(swell)}$  described in SAN, atrial, and ventricular cells [for review, see refs 19–21]. We thus conclude that  $I_{Cl(swell)}$  is present in cardiac Purkinje cells of the rabbit.

In cardiac cells, other  $Cl^-$  currents are also found. These include the  $Ca^{2+}$ -activated  $Cl^-$  current ( $I_{Cl(Ca)}$ ) [28], the cystic fibrosis transmembrane conductance regulator  $Cl^-$  current ( $I_{Cl(CFTR)}$ ) [29, 30], the anionic background current ( $I_{AB}$ ) [31], and the inwardly rectifying  $Cl^-$  current ( $I_{Cl(ir)}$ ) [32]. These currents could potentially have interfered with our measurements. However, we have a number of reasons to believe that the role of these  $Cl^-$  currents in our study was limited. First,  $I_{Cl(swell)}$ ,  $I_{Cl(Ca)}$ , and  $I_{Cl(ir)}$  have very distinct I-V characteristics.  $I_{Cl(swell)}$  exhibits outward rectification [1–3], whereas  $I_{Cl(ir)}$  exhibits inward rectification and is active at hyperpolarized membrane potentials [32], and  $I_{Cl(Ca)}$  has a bell-shaped I-V relationship and is active at membrane potentials positive to  $-40$  mV [28]. Second,  $I_{Cl(Ca)}$  inactivates completely within 50 ms upon depolarization, while  $I_{Cl(CFTR)}$  is not active at all in the absence of agonists [29, 30]. Finally, stilbene derivatives do not inhibit  $I_{Cl(CFTR)}$ ,  $I_{Cl(ir)}$ , and  $I_{AB}$ , while they block  $I_{Cl(swell)}$  at concentrations of 0.1 mM and higher [19, 20, 31, 32]. Taken together, we believe that the hypotonicity-induced current we investigated in this study represents  $I_{Cl(swell)}$  rather than  $I_{Cl(Ca)}$ ,  $I_{AB}$ ,  $I_{Cl(CFTR)}$ , or  $I_{Cl(ir)}$ .

### Significance of $I_{Cl(swell)}$ for Purkinje cell electrophysiology

In our experiments, the calculated  $E_{Cl}$  was  $-50$  mV. During the normal Purkinje cell action potential, the membrane potential ranges between  $-80$  and  $+40$  mV (cf. table 1). Thus  $Cl^-$  channels have the unique ability to contribute both inward and outward currents during the Purkinje action potential. In Purkinje cells, we observed that activation of  $I_{Cl(swell)}$  produces a small depolarization of the RMP and accelerated repolarization during phase 1 and phase 2, which leads to action potential shortening (fig. 1, table 2). These findings are in agreement with findings in ventricular cells of dog, rabbit, and guinea pig [8, 13–15]. In addition, we found that the magnitude of these effects increased with increasing magnitude of the  $Cl^-$  conductance, which agrees with findings in rabbit ventricular cells [8]. Apart from activation of  $I_{Cl(swell)}$ , changes in other membrane conductances may also contribute to the observed action potential shortening and RMP depolarization in response to the hypotonic solutions. Changes in L-type  $Ca^{2+}$  current,  $Na^+$ - $Ca^{2+}$  exchange current, and the slow component of the delayed rectifier  $K^+$  current have been reported in response to cell swelling [14, 33, 34]. In our experiments, however, the  $I_{Cl(swell)}$  antagonist DIDS [19, 20] largely inhibited the effects of swelling on the action potential configuration, indicating that  $I_{Cl(swell)}$  was the main cause of the action potential shortening and RMP depolarization.

The ability of  $I_{Cl(swell)}$  to depolarize cardiac cells is opposed by the presence of the background  $K^+$  conductance that normally controls the RMP [20]. Purkinje cells typically exhibit a low inward rectifier  $K^+$  current ( $I_{K1}$ ) density compared to ventricular cells [22, 23]. In such cells,

activation of  $I_{Cl(swell)}$  was proposed to cause a large depolarization, conceivably leading to the development of spontaneous activity [35, 36]. In the present study, however, abnormal automaticity was never observed, not even when the extracellular tonicity was as low as 135 mOsm (fig. 1). This finding is similar to observations made in atrial cells [17], which also have a low  $I_{K1}$  density [37]. Du and Sorota [17] found that the RMP depolarization during swelling was larger in atrial than in ventricular cells, but no ectopic activity was observed. Apart from differences in  $I_{K1}$  density, differences in  $I_{Cl(swell)}$  density [5, 6] and response to swelling [1] may also be involved in the more profound depolarization of the atrial cells. Activation of time-independent  $Cl^-$  conductances has also been proposed to result in early afterdepolarizations (EADs) [20]. This has indeed been demonstrated, both in a model study [38] and in isolated ventricular cells [39]. However, the EADs were only found when  $E_{Cl}$  was positive to  $-30$  mV [38, 39] or when  $[K^+]_o$  was lowered to 2 or 3 mM [39]. In our experiments, where  $E_{Cl}$  was  $-50$  mV and  $[K^+]_o$  was 5.4 mM, EADs were not observed. Activation of  $I_{Cl(swell)}$  does not induce ectopic activity, i.e., abnormal automaticity or triggered activity, in cardiac Purkinje cells, but it does cause RMP depolarization and action potential shortening. These two effects facilitate the development of reentrant arrhythmias [for review, see refs 20, 21]. During ischemia-reperfusion, cell swelling occurs [40]. Consequent activation of  $I_{Cl(swell)}$  may thus be an important factor favoring the occurrence of arrhythmias associated with this pathological condition.  $Cl^-$  current blockade may therefore be potentially antiarrhythmogenic.

### Limitations of the study

The effects of swelling on Purkinje action potential configuration were measured in a 'modified' Tyrode's solution in which the  $Na^+$  concentration was lowered to 55 mM. Variable amounts of sucrose were then added to obtain solutions of 300, 210, or 135 mOsm. Using these modified Tyrode's solutions, cells produce action potentials. However, action potential duration was decreased significantly (table 1). This action potential shortening may have implications for the inducibility of EADs. Zeng and Rudy [41] showed that the incidence of EADs was higher for longer action potentials. Furthermore, the reduction of  $[Na^+]_o$  may have reduced the window  $Na^+$  current, which is important for generation of abnormal automaticity [42]. Therefore, in our study, the inducibility of EADs and abnormal automaticity may have been decreased.

- 1 Sorota S. (1992) Swelling-induced chloride-sensitive current in dog atrial cells revealed by whole cell patch clamp method. *Circ. Res.* **70**: 679–687
- 2 Tseng G. N. (1992) Cell swelling increases membrane conductance of canine cardiac cells: evidence for a volume-sensitive  $Cl$  channel. *Am. J. Physiol.* **262**: C1056–C1068

- 3 Hagiwara N., Masuda H., Shoda M. and Irisawa H. (1992) Stretch-activated anion currents of rabbit cardiac myocytes. *J. Physiol.* **456**: 285–302
- 4 Clemo H. F. and Baumgarten C. M. (1997) Swelling-activated  $Gd^{3+}$ -sensitive cation current and cell volume regulation in rabbit ventricular myocytes. *J. Gen. Physiol.* **110**: 297–312
- 5 Vandenberg J. I., Yoshida A., Kirk K. and Powell T. (1994) Swelling-activated and isoprenaline-activated chloride currents in guinea pig cardiac myocytes have distinct electrophysiology and pharmacology. *J. Gen. Physiol.* **104**: 997–1017
- 6 Oz M. C. and Sorota S. (1995) Forskolin stimulates swelling-induced chloride current, not cardiac cystic fibrosis transmembrane-conductance regulator current, in human cardiac myocytes. *Circ. Res.* **76**: 1063–1070
- 7 Clemo H. F., Stambler B. S. and Baumgarten C. M. (1999) Swelling-activated chloride current is persistently activated in ventricular myocytes from dogs with tachycardia-induced congestive heart failure. *Circ. Res.* **84**: 157–165
- 8 Borren M. M. G. J. van, Verkerk A. O., Vanharanta S. K., Baartscheer A., Coronel R. and Ravesloot J. H. (2002) Reduced swelling activated  $Cl^-$  current densities in hypertrophied ventricular myocytes of rabbits with heart failure. *Cardiovasc. Res.* **53**: 869–878
- 9 Sorota S. and Du X.-Y. (1998) Delayed activation of cardiac swelling-induced chloride current after step changes in cell size. *J. Cardiovasc. Electrophysiol.* **9**: 825–831
- 10 Shuba L. M., Ogura T. and McDonald T. F. (1996) Kinetic evidence distinguishing volume-sensitive chloride current from other types in guinea-pig ventricular myocytes. *J. Physiol.* **491**: 69–80
- 11 Desilets M. and Baumgarten C. M. (1986)  $K^+$ ,  $Na^+$ , and  $Cl^-$  activities in ventricular myocytes isolated from rabbit heart. *Am. J. Physiol.* **251**: C197–C208
- 12 Vaughan-Jones R. D. (1979) Non-passive chloride distribution in mammalian heart muscle: micro-electrode measurements of the intracellular chloride activity. *J. Physiol.* **295**: 83–109
- 13 Vandenberg J. I., Bett G. C. and Powell T. (1997) Contribution of a swelling-activated chloride current to changes in the cardiac action potential. *Am. J. Physiol.* **273**: 541–547
- 14 Li G.-R., Zhang M., Satin L. S. and Baumgarten C. M. (2002) Biphasic effects of cell volume on excitation-contraction coupling in rabbit ventricular myocytes. *Am. J. Physiol. Heart. Circ. Physiol.* **282**: H1270–H1277
- 15 Zaza A., Rocchetti M., Piazza S., Armato A. and Cavalieri B. (1998) Swelling-induced current in rabbit sinoatrial myocytes: role in modulating of pacemaking. *Pflügers. Arch.* **436**: R16
- 16 Lei M. and Kohl P. (1998) Swelling-induced decrease in spontaneous pacemaker activity of rabbit isolated sino-atrial node cells. *Acta. Physiol. Scand.* **164**: 1–12
- 17 Du X.-Y. and Sorota S. (1997) Cardiac swelling-induced chloride current depolarizes canine atrial myocytes. *Am. J. Physiol.* **272**: H1904–H1916
- 18 Bénitah J. P., Gomez A. M., Delgado C., Lorente P. and Lederer W. J. (1997) A chloride current component induced by hypertrophy in rat ventricular myocytes. *Am. J. Physiol.* **272**: H2500–H2506
- 19 Sorota S. (1999) Insights into the structure, distribution and function of the cardiac chloride channels. *Cardiovasc. Res.* **42**: 361–376
- 20 Hume J. R., Duan D., Collier M. L., Yamazaki J. and Horowitz B. (2000) Anion transport in heart. *Physiol. Rev.* **80**: 31–81
- 21 Hiraoka M., Kawano S., Hirano Y. and Furukawa T. (1998) Role of cardiac chloride currents in changes in action potential characteristics and arrhythmias. *Cardiovasc. Res.* **40**: 23–33
- 22 Verkerk A. O., Veldkamp M. W., Abbate F., Antoons G., Bouman L. N., Ravesloot J. H. et al. (1999) Two types of action potential configuration in single cardiac Purkinje cells of sheep. *Am. J. Physiol.* **277**: H1299–H1310

- 23 Cordeiro J. M., Spitzer K. W. and Giles W. R. (1998) Repolarizing  $K^+$  currents in rabbit Purkinje cells and ventricular cells. *J. Physiol.* **503**: 811–823
- 24 Huelsing D. J., Spitzer K. W., Cordeiro J. M. and Pollard A. E. (1998) Conduction between isolated rabbit Purkinje and ventricular myocytes coupled by a variable resistance. *Am. J. Physiol.* **274**: H1163–H1173
- 25 Draper M. H. and Weidmann S. (1951) Cardiac resting and action potentials recorded with an intracellular electrode. *J. Physiol.* **115**: 74–94
- 26 Hauswirth O., Noble D. and Tsien R. W. (1972) The dependence of plateau currents in cardiac Purkinje fibres on the interval between action potentials. *J. Physiol.* **222**: 27–49
- 27 Dangman K. H., Dresdner K. P. and Michler R. E. (1988) Transmembrane action potentials and intracellular potassium activity of baboon cardiac tissues. *Cardiovasc. Res.* **22**: 202–212
- 28 Zygmunt A. C. and Gibbons W. R. (1991) Calcium-activated chloride current in rabbit ventricular myocytes. *Circ. Res.* **68**: 424–437
- 29 Harvey R. D. and Hume J. R. (1989) Autonomic regulation of a chloride current in heart. *Science* **244**: 983–985
- 30 Bahinski A., Nairn A. C., Greengard P. and Gadsby D. C. (1989) Chloride conductance regulated by cyclic AMP-dependent protein kinase in cardiac myocytes. *Nature* **340**: 718–721
- 31 Spencer C. I., Uchida W. and Kozlowski R. Z. (2000) A novel anionic conductance affects action potential duration in isolated rat ventricular myocytes. *Br. J. Pharmacol.* **129**: 235–238
- 32 Duan D., Ye L., Britton F., Horowitz B. and Hume J. R. (2000) A novel anionic inward rectifier in native cardiac myocytes. *Circ. Res.* **86**: e63–e71
- 33 Sasaki N., Mitsuiye T., Wang Z. and Noma A. (1994) Increase of the delayed rectifier  $K^+$  and  $Na^+-K^+$  pump currents by hypotonic solutions in guinea-pig cardiac myocytes. *Circ. Res.* **75**: 887–895
- 34 Wright A. R., Rees S. A., Vandenberg J. I., Twist V. M. and Powell T. (1995) Effects of hypo-osmotic stress on sodium-calcium exchange in isolated guinea-pig ventricular myocytes. *J. Physiol.* **488**: 293–301
- 35 Ackerman J. M. and Clapham D. E. (1993) Cardiac chloride channels. *Trends Cardiovasc. Med.* **3**: 23–28
- 36 Harvey R. D. (1996) Cardiac chloride currents. *News Physiol. Sci.* **11**: 175–181
- 37 Hume J. R. and Uehara A. (1985) Ionic basis of the different action potential configurations of single guinea-pig atrial and ventricular myocytes. *J. Physiol.* **368**: 525–544
- 38 Riemer T. L., Sobie E. A. and Tung L. (1998) Stretch-induced changes in arrhythmogenesis and excitability in experimentally based heart cell models. *Am. J. Physiol.* **275**: H431–H442
- 39 Yamawake N., Hirano Y., Sawanobori T. and Hiraoka M. (1992) Arrhythmogenic effects of isoproterenol-activated  $Cl^-$  current in guinea-pig ventricular myocytes. *J. Mol. Cell. Cardiol.* **24**: 1047–1058
- 40 Tranum-Jensen J., Janse M. J., Fiolet W. T., Krieger W. J., D'Almoncourt C. N. and Durrer D. (1981) Tissue osmolality, cell swelling, and reperfusion in acute regional myocardial ischemia in the isolated porcine heart. *Circ. Res.* **49**: 364–381
- 41 Zeng J. and Rudy Y. (1995) Early afterdepolarizations in cardiac myocytes: mechanism and rate dependence. *Biophys. J.* **68**: 949–964
- 42 Janse M. J. (1992) The premature beat. *Cardiovasc. Res.* **26**: 89–100



To access this journal online:  
<http://www.birkhauser.ch>

---